Published in final edited form as:
Cryobiology. 2010 December ; 61(3): 280–288. doi:10.1016/j.cryobiol.2010.09.006.

Pre-Conditioning Cryosurgery: Cellular and Molecular Mechanisms and Dynamics of TNF-α Enhanced Cryotherapy in an *in vivo* Prostate Cancer Model System

Jing Jiang[1], **Raghav Goel**[1], **Stephen Schmechel**[2], **Gregory Vercellotti**[3], **Colleen Forster**[5], and **John Bischof**[1,4]

[1] Departments of Biomedical Engineering, University of Minnesota, Minneapolis, Minnesota, MN 55455, USA

[2] Laboratory Medicine and Pathology, University of Minnesota, Minneapolis, Minnesota, MN 55455, USA

[3] Medicine, University of Minnesota, Minneapolis, Minnesota, MN 55455, USA

[4] Mechanical Engineering and Urologic Surgery, University of Minnesota, Minneapolis, Minnesota, MN 55455, USA

[5] BioNet, University of Minnesota, Minneapolis, Minnesota, MN 55455, USA

Abstract

Cryosurgery is increasingly being used to treat prostate cancer; however, a major limitation is local recurrence of disease within the previously frozen tissue. We have recently demonstrated that tumor necrosis factor alpha (TNF-α), given 4 hours prior to cryosurgery can yield complete destruction of prostate cancer within a cryosurgical iceball. The present work continues the investigation of the cellular and molecular mechanisms and dynamics of TNF-α enhancement on cryosurgery. *In vivo* prostate tumor (LNCaP Pro 5) was grown in a dorsal skin fold chamber (DSFC) on a male nude mouse. Intravital imaging, thermography, and post-sacrifice histology and immunohistochemistry were used to assess iceball location and the ensuing biological effects after cryosurgery with and without TNF-α pre-treatment. Destruction was specifically measured by vascular stasis and by the size of histologic zones of injury (i.e. inflammatory infiltrate and necrosis). TNF-α induced vascular pre-conditioning events that peaked at 4 hours and diminished over several days. Early events (4 – 24 hours) include upregulation of inflammatory markers (nuclear factor-κB (NFκB) and vascular cell adhesion molecule-1 (VCAM)) and caspase activity in the tumor prior to cryosurgery. TNF-α pre-conditioning resulted in recruitment of an augmented inflammatory infiltrate at day 3 post treatment vs. cryosurgery alone. Finally, preconditioning yielded enhanced cryosurgical destruction up to the iceball edge at days 1 and 3 vs. cryosurgery alone. Thus, TNF-α pre-conditioning enhances cryosurgical lesions by vascular mechanisms that lead to tumor cell injury via promotion of inflammation and leukocyte (esp. neutrophil) recruitment.

[*]Corresponding author (Reprint requests should be sent to): John. C. Bischof, Ph.D., Professor, Department of Mechanical Engineering, University of Minnesota, Minneapolis MN 55455, Ph: 612-625-5513, bischof@umn.edu.

Keywords

prostate cancer; cryosurgery; TNF-α; caspase; NFκB

Introduction

Prostate cryosurgery using intra-operative iceball imaging and modern Argon Joule-Thomson probe technology has increased markedly in the last decade [45,47]. Although mostly accepted for salvage following local radiotherapy failure, it is now increasingly used as a primary treatment for locally advanced disease [29]. It is estimated that 6,680 cryoablation procedures were performed in the United States in 2005 with 15,000 procedures projected in 2010 [13]. Five-year biochemical disease free status for cryosurgery is now comparable to published results for radiation and surgery in the prostate [27]. However, reproducible clinical application of cryosurgery continues to suffer from the inability of the technique to destroy cells at the periphery of the lesion (i.e. at the iceball edge) where the temperatures are above −40°C [16]. Clearly, sub-lethal injury at the iceball edge may lead to cancer recurrence. However, over-freezing (creating an iceball beyond clinically apparent cancer) may result in damage of surrounding normal structures such as nerves and vessels, leading to complications [49]. As both under and over-freezing outcomes are undesirable, much research has focused on controlling destruction within the iceball by cellular, vascular and immunological mechanisms [4,6,17,46]. It is now clear that one important approach to controlling disease at the edge of the prostate, where both the cancer and the iceball edge co-exist, is to augment these mechanisms with cryosurgical adjuvants as recently reviewed [19].

Several molecular adjuvants have been used to enhance cryosurgical injury within the iceball. These adjuvants can be broadly categorized into four groups: 1) thermophysical adjuvants to enhance the injury by ice crystal formation, 2) chemotherapeutic approaches to induce apoptosis (programmed cell death), 3) intravascular agents to induce vessel damage (and therefore ischemic necrosis), and 4) immunomodulators to stimulate immune-mediated tumor damage [19]. We have previously demonstrated that pre-treatment with TNF-α, a vascular agent, can completely destroy tumor throughout a cryosurgical iceball [20,26].

TNF-α, isolated 30 years ago, is a multifunctional cytokine that plays a key role in apoptosis and cell survival as well as in inflammation and immunity. There are a number of mechanisms by which TNF-α can induce an anticancer effect, including: apoptosis [44], pro-coagulation and acute hemorrhagic necrosis [23], activation and mediation of macrophage and natural killer (NK) cell destruction [23], and occasionally the initiation of tumor specific immunity [3,22,37]. Our earlier results suggest that inflammation and vascular injury are critical specifically to TNF-α-mediated enhancement of cryosurgery [26]. However, further description of the timing and mechanisms of TNF-α pre-conditioning and enhancement of combinatorial treatment are needed for optimal translation to clinical use.

This work specifically investigates and reports on the time course and mechanism of TNF-α pre-treatment effects in tumors, and of combinatorial treatment (TNF-α pre-treatment + cryosurgery). While the systemic use of native TNF-α yields toxicity, we are able to topically apply it in the dorsal skin fold chamber without toxicity in this work. In other work we have also shown that safe systemic delivery is possible followed by cryosurgery with a gold nanoparticle carrier (CYT-6091) which may ultimately translate to clinical use [20]. Enhancement of cryosurgical injury in combinatorial treatment by histology is confirmed here as previously reported [4,20,25]. In addition, we show for the first time that enhancement is accompanied by the presence of a strong and sustained neutrophil

inflammatory infiltrate. Also, new immunohistochemical results show that TNF-α-mediated enhancement correlates with translocation of NFκB, VCAM expression and upregulated expression of caspase 3 (a marker of apoptosis) in the cells and vasculature of the tumor.

Materials and Methods

Cell culture

LNCaP Pro 5 cells were transfected with plasmid DNA encoding the DsRed-express (Clontech, Mountain View, CA) fluorescent protein to permit monitoring of tumor growth in dorsal skin fold chambers (DSFCs) as described previously [20]. DsRed-LNCaP cells were cultured as adherent monolayers in Dulbecco's modified Eagle's medium (DMEM)/F12 media (BD Biosciences, San Jose, CA) supplemented with 10% of fetal bovine serum, antibiotics, and 10^{-9} mol/L dihydrotestosterone (DHT) as previously described [4].

Animals

Athymic male NU/J mice were obtained from the Jackson Laboratory (Bar Harbor, ME) and housed according to an approved IACUC and University-approved standard operating procedures. Experiments were performed when mice were 6–8 weeks old. Animals with DSFCs were housed under conditions of higher humidity and temperature than normal to maintain tissue microvasculature [20]. When appropriate, animals were anesthetized by an i.p. injection of ketamine (100 mg/kg) and xylazine (10 mg/kg).

DSFC and tumor cell implantation

A DSFC was implanted in each nude mouse as previously described [20,24]. Immediately after DSFC implantation and on day 4 after implantation, DsRed-LNCaP cells (1-2 million cells/mouse; suspended in 30 μL Matrigel (BD Biosciences, San Jose, CA) that had been diluted 3:1 in serum-free medium) were seeded into the DSFC chamber window. Intravital imaging of tumor cells was performed using a Nikon inverted fluorescent microscope equipped with a 20× objective (Nikon, Melville, NY) and silicon intensified transmission camera (Hamamatsu, Bridgewater, NJ) as previously described [4,24,43]. Experiments were performed on day 12 following DSFC implantation, when tumor cells were found to cover the entire chamber window as previously reported [4,20,26].

Treatment with TNF-α, NFκB inhibitor, and cryosurgery

On the day of the study, the glass windows of DSFCs were removed. The NFκB inhibitor Bay 11-7085 (EMD Biosciences, San Diego, CA; dissolved in dimethyl sulfoxide (Me2SO) at 10 mg/ml) was topically applied in the DSFC at a dose of 0.4 mg/kg for 15 min. After Bay treatment, or without pre-treatment with Bay, 200 ng/mouse of TNF-α (a gift from CytImmune Science, Inc., Rockville, MD; dissolved in 30 μl saline), or a sham mixture of saline, were topically applied for 15 min. The glass windows were replaced and animals were treated with cryosurgery 4 hours later as described previously [20,26]. Briefly, DSFC windows were removed and a 1 mm diameter brass extension tip fitted to a 5 mm cryoprobe (Endocare, Irvine, CA) was inserted into the center of the DSFC for 55 s (to attain temperatures of −100°C) followed by passive thawing at room temperature. The temperature was monitored throughout the procedure by the use of infrared thermography and thermocouples placed at 2, 3 and 4 mm radial positions around the DSFC center [20].

Intravital measurements of vascular flow

On days 1, 3 or 7 following cryosurgery (with or without prior TNF-α pre-treatment), 0.1 ml of 10 mg/ml 70-kDa FITC-labeled dextran (Sigma, St. Louis, MO) was injected into the tail vein of each animal. Using the inverted fluorescent microscope and camera described above,

the average radius of signal in the FITC channel was measured at four perpendicular radial directions relative to the chamber center. Vascular stasis was defined as the lack of fluorescence signal (signifying lack of blood flow, or perfusion defect). Leukocyte interactions with vascular endothelium were visualized following injection of 10 ml/kg body weight of saline containing 1 mg/ml of the nuclear dye rhodamine 6G (Sigma, St. Louis, MO), which labeled leukocyte nuclei intravitally [10]. Slow moving/rolling leukocytes near microvessel walls and fast moving leukocytes in central vascular flow were videotaped during their passage through vessels with a 20× objective using the imaging set up described above.

Histology and immunohistochemistry

Animals were sacrificed 4 hours post TNF-α treatment or at day 1, 3 and 7 post cryosurgery immediately after vascular imaging. The entire tumor tissue from the viewing area of the dorsal skin fold chamber was bisected: one-half of each specimen was fixed in 10% buffered formalin (Sigma, St. Louis, MO), embedded in paraffin, sectioned at 4-7 μm and stained with hematoxylin-eosin (H&E). The other half was frozen and stored at −80 °C for immunohistochemistry (IHC). Cryostat sections were acetone-fixed, blocked with serum and incubated with optimal dilutions of anti-mouse antibodies. NFκB p65 (Gene Tex, Inc., Ivrine, CA) and VCAM (Vector Laboratories, Burlingame, CA) primary antibodies were used for staining of specific molecules. This was followed by ASA-horseradish peroxidase (Covance, Dedham, MA) application and finally 3,3′-Diaminobenzidine (DAB) chromagen that yields a brown color reaction. CD31/PECAM (Biocare Medical, Concord, CA) for endothelial cells and caspase 3 (Biocare Medical, Concord, CA) primary antibodies were co-stained, and dual chromogen imaging was used for CD31/PECAM (Biocare Medical) and caspase 3 (Biocare Medical) to co-localize apoptosis and endothelium.

Histologic sections were digitized using a whole slide digital imaging system, ScanScope (Aperio, Vista, CA), and analyzed using Spectrum software (Aperio, Vista, CA). From prints of whole slide images, distinct histologic layers corresponding to the zones of central necrosis, inflammation, thrombosis/ischemic necrosis, granulation tissue and viable tumor were measured and averaged. Measurements were performed at angles of 30°, 60° and 90° relative to a plane perpendicular to the long axis of the mouse (which was the plane of bisection of tissue pieces removed from each DSFC). Shrinkage was found to be uniform and accounted for as previously reported [20], yielding an average of 18.9 ± 7.7% at each radial location. For quantification of VCAM and caspase 3 IHC staining intensity, digital annotation regions were applied in representative areas of each tumor section and pixels that exceeded threshold limits were quantified (as a ratio of total) using Positive Pixel Count v9 software (Aperio, Vista, CA). NFκB activation was characterized by the translocation of the p65 (labeled with brown precipitate) from the cytoplasm to nucleus and presented as number of NFκB activated cells / number of total cells in the representative areas.

Statistics

Statistical significance was determined using the paired student’s t test. If the difference was at the level of $p<0.05$, it was determined significant. Otherwise, the difference between two measurements was not significant, i.e., $p>0.05$.

Results

Histological zones following cryosurgery without TNF-α

The maximum cryosurgical lesion without TNF-α pre-treatment presented at day 3. Cryoinjury was characterized by five histological zones extending radially outward from the probe location (Fig. 1). Zone 1: immediately surrounding the cryoprobe a central necrotic

zone was formed, characterized by intense eosinophilic staining of cells, loss of hematoxylin staining and loss of cellular detail. Blood vessels in this central necrotic zone were destroyed. In some specimens, scattered neutrophils were present in this zone. Zone 2: surrounding the central necrotic zone, a marked band of inflammation was present. Neutrophils were the dominant cells in this band, with lesser numbers of lymphocytes and histocytes also present. Zone 3: centrifugal to the inflammatory band was a zone of thrombosis and resulting hemorrhage and ischemic necrosis. Zone 4: surrounding the zone of thrombosis/ischemic necrosis was a zone of granulation tissue characterized by fibroblast/myofibroblast infiltration and proliferation, new collagen deposition and nascent capillary formation [59]. The granulation tissue zone was found only on day 3 and later. The five zones from central necrosis to granulation tissue were defined as the cryolesion. Zone 5: Peripheral to the cryolesion was a zone of viable tumor.

TNF-α pre-conditioning is mediated at the vascular level

Histological features following topical TNF-α treatment were analyzed. Acute vascular injury events, including microvascular dilatation, thrombosis/congestion and hemorrhage (Fig. 2A) were first observed and reached the maximum as early as 4 hours after TNF-α treatment and notably decreased from day 1 to day 7. An acute inflammatory response was observed at 4 hours, characterized by an influx of neutrophils, many adherent to the endothelial layer and infiltrating into the interstitial space (Fig. 2B). Later, tumor cell necrosis in some areas with thrombosis/congestion became notable and peaked between day 1 and 3, likely due to diminished blood supply and cytotoxic effects of the inflammatory infiltrate. These histological observations are summarized in Table 1. Immunohistochemistry of these same samples revealed that TNF-α treatment alone induced NFκB and caspase 3 activity 4 hours after administration ($p<0.05$), although both were suppressed later at 24 hours (Fig. 2C). VCAM expression was increased over the same period, although the changes were not statistically significant.

Histologic evolution of cryolesion zones and TNF-α modification of evolution

One day after cryosurgery, the small central necrosis zone and a surrounding large zone of scant inflammation and thrombosis were difficult to distinguish by H&E staining. Blood vessels were severely damaged at the center, evidenced by fibrin deposition within vessels and extravasation of erythrocytes. Toward the edge of the cryolesion, vascular damage was less severe, characterized by microvascular dilatation. Viable tumor was present in this zone at day 1, such that it was difficult to distinguish the cryolesion edge. No significant TNF-α enhancement was notable at day 1. At day 3, the cryolesion histologic zones were established, including a marked band of inflammation, chiefly neutrophils, surrounding the central necrotic zone, and early granulation tissue formation. At day 3, the radius of the histologically identified cryolesion correlated well with the radius of the vascular stasis visualized by intravital imaging (Fig. 4, Table 2). TNF-α significantly enlarged the cryolesion radius from 3.3 ± 0.6 to 4.3 ± 0.3 mm by histology (Fig. 3C, Table 2). Specific zones were also enhanced by TNF-α. The inflammatory zone was significantly increased by TNF-α, from 1.9 ± 0.8 mm with cryosurgery alone to 3.0 ± 0.5 mm with combined TNF-α pre-treatment followed by cryosurgery (Fig. 3C, Table 2). Further, a thin zone of granulation tissue (0.6 ± 0.5 mm in width) peripheral to the zone of thrombosis/ischemic necrosis was formed at day 3 following combinatorial therapy, which was not clearly formed after cryosurgery alone (Fig. 3C Table 2). At day 7, the inflammatory and granulation tissue zones continued to expand. Granulation tissue became notable with cryosurgery treatment alone (0.8 ± 0.3 mm in width) and was expanded centripetally into the ischemic necrosis layer with TNF-α pre-treatment (1.2 ± 0.5 mm in width) (Fig. 3C, Table 2). Importantly, pre-treatment of TNF-α completely destroyed the tumor tissue up to the iceball edge (3.9 mm, −0.5°C) at day 1 and 3, which could not be achieved by cryosurgery alone.

Intravital imaging evaluation of TNF-α enhanced vascular injury

The stasis radius modified by TNF-α post cryosurgery was measured by FITC-dextran fluorescence at day 1, 3 and 7 post cryosurgery in both tumor tissue and normal skin (Fig. 4, Table 2). With cryosurgery alone, the stasis radius increased from 2.7 ± 0.7 mm at day 1 to 3.3 ± 0.5 mm at day 3 ($p<0.05$) and 3.1 ± 0.1 mm at day 7 in tumor tissue. Whereas, with TNF-α pre-treatment, a large stasis radius was already created at day 1 (3.8 ± 0.8 mm) which remained large at day 3 (4.0 ± 0.4 mm) and day 7 (3.7 ± 0.5 mm). Pre-treatment with TNF-α was observed to increase stasis radius up to the edge of the iceball (3.9 mm) at all time points (day 1, 3 and 7) after cryosurgery compared with cryosurgery alone. This observation was consistent with our previous observation at day 3 post cryosurgery [20,24], suggesting enhanced vascular damage post cryosurgery induced by TNF-α pre-treatment in tumor. On the other hand, the normal skin showed significant contraction of the radii of vascular stasis from day 1 through day 7 after cryosurgery both with and without TNF-α pre-treatment. TNF-α pre-treatment followed by cryosurgery in normal skin, yielded a larger vascular stasis early on (day1 and 3) ($p<0.05$), with a faster reduction in stasis radius at day 7 (1.0 ± 0.3 mm) compared with cryosurgery alone (2.1 ± 0.4 mm) ($p<0.05$). This suggests an enhanced wound healing process induced by TNF-α in normal skin possibly through enhanced blood flow post freezing.

Molecular and cellular mechanisms of TNF-α enhanced cryosurgery

NFκB translocation, VCAM expression and caspase 3 signaling pathway induction were altered due to treatment as assessed by IHC at day 1 after cryosurgery with and without TNF-α pre-treatment (Fig. 5A & B). NFκB translocation and VCAM expression were significantly activated in tumor, endothelial, and the occasional fibroblast cell. Caspase 3 signaling was upregulated in infiltrating leukocytes and endothelial cells. These effects are enhanced by TNF-α pre-treatment at the edge of the cryolesion. At day 3 post cryosurgery, these molecular events decreased to the point where no signal was seen by IHC (data not shown). Upregulation of VCAM and NFκB in combinatorial therapy appeared to have a greater biological effect on the lesion as shown in Fig. 5C & D. Specifically, within the dense inflammatory band, TNF-α pre-treatment greatly enhanced the density of neutrophils infiltrating the tissue from 54.6 ± 18.2 to 121.7 ± 53.3 cells/field ($p<0.05$, Fig. 5D) in the inflammation band. The TNF-α enhanced inflammatory response at day 3 post combinatorial cryosurgery was likely due to VCAM expression mediated by NFκB since the inflammatory infiltrate was significantly reduced with use of the NFκB inhibitor Bay, from 121.7 ± 53.3 cells/field without Bay to 40.1 ± 20.5 cells/field with Bay (Fig. 5D). This inflammatory infiltrate can also lead to caspase activation in some neutrophils and endothelial cells at day 1 (Fig. 5B). Together, these inflammatory and subsequent caspase mediated events lead to the extension of the cryosurgical lesion with TNF-α.

Discussion

In recent years a new research thrust has emerged in cryosurgery that focuses on the use of molecular adjuvants to manipulate and enhance cellular and tissue cryodestruction [2,6,20,41,56]. The usage of these cryoadjuvants was recently reviewed in [19]. For instance, as apoptosis is recognized as a mode of cell death at the periphery of the iceball, many studies used apoptosis inducers (chemotherapeutics) combined with cryosurgery at milder temperature (−40 to −0.5°C) [5,7,14,15,33,40,61]. However, most of these studies are *in vitro* and their impact in vivo still requires verification. Importantly, no adjuvant except the pro-inflammatory cytokine TNF-α, has demonstrated the ability to extend cryosurgical destruction *in vivo* up to the iceball edge (−0.5 °C) [20,21,24]. The present work is an extension of these previous studies to more completely study the complicated effects of TNF-α enhancement on tumor tissue. Specifically, TNF-α can activate both

inflammatory and apoptotic intracellular pathways. Thus, the exact cellular and molecular mechanisms and timing of TNF-α pre-conditioning events and ensuing cryosurgical enhancement are poorly understood and continue to be investigated in this study. Here we show for the first time that the presence of a sustained neutrophil infiltrate at the cellular level is important to this enhancement. In addition, our data shows that both inflammatory and apoptotic pathways participate at the molecular level in providing cryosurgical injury enhancement, although the inflammatory pathway appears to dominate the response as only it can be blunted by NFκB inhibition [26].

A major challenge of studying the enhanced mechanisms of by TNF-α or other cryoadjuvants *in vivo* is the differential spatial and temporal injury response as a function of the temperature response, especially related to the iceball edge, within the tissue. Therefore, in this study, we show the distribution of the cellular and molecular activity in tissue using a DSFC model that allows temperature monitoring and quantification of injury responses over time (day 1, 3 and 7) after treatment. Five histological zones were observed post cryosurgery, including central necrosis, inflammation, thrombosis/ischemic necrosis, granulation and viable tumor. TNF-α spatial and temporal modification of these zones and the early molecular mechanisms that affect this response were studied.

Our results suggest that the inflammatory infiltrate is the main mechanism of TNF-α cryoinjury enhancement. Recent evidence has shown that host mediated injury, including vascular and immunological effects, define the edge of a cryosurgical lesion [17,50]. The host response is orchestrated by the innate immune system in a non-antigen specific manner. Key elements of the host response are: to destroy tumor cells, prevent the spread of tissue damage, contain imbalances of homeostasis, remove dead damaged/altered tissue, and ultimately restore tissue function [31]. The inflammatory infiltrate is an important part of this host response. The interaction of the host response with the local tumor tissue usually takes place during ischemia reperfusion post cryosurgery [18,38]. Local tissue damage yields “danger signals”, including the synthesis of pro-inflammatory cytokines (e.g. TNF-α, IL-1 and 6) and chemokines that initiate recruitment of circulating leukocytes to the injury site [48]. Reperfusion and subsequent re-oxygenation after freeze thaw induce NFκB-dependant transcription of gene encoding adhesion molecules (ICAM, VCAM, E-selectins and P-selectins) and chemokines [1,9,58] that further mediate leukocyte transendothelium migration from circulation to the interstitium. Neutrophils play a central role in this host response by initiating the coagulation cascade [54], acting as chemoattractants for inflammatory cells [11,54], beginning the debridement of devitalized tissue, and phagocytosis of foreign bodies by releasing toxic agents (reactive oxygen species, cationic peptides, eicosanoids and proteases) [60].

Our work suggests that the main effect of TNF-α is to pre-condition the vasculature by activating vascular endothelial cells to recruit inflammatory cells and promote their extravasation. Our results are consistent with published work [31,42]; however the connection to cryosurgery is new in this work. Vascular pre-conditioning is mediated by NFκB pathway activation, which peaked at 4 hours, and led to expression of adhesion molecules (VCAM) and adhesion of leukocytes at endothelial surfaces. Combined with cryosurgery, both NFκB translocation and VCAM activation were significantly enhanced by TNF-α pre-treatment at day 1 (Fig. 5B), suggesting that TNF-α pre-treatment mediates later augmented inflammatory infiltration at day 3 post cryosurgery (Fig. 5C & D).

In addition, endothelial apoptosis and increased vascular permeability for blood constituents (i.e. cells, proteins) is observed after TNF-α application. This may be either due to TNF-α receptor binding on endothelial cells and caspase activation, and/or reactive oxygen species from pre-recruited inflammatory cells by TNF-α. Finally, infiltrated leukocytes (neutrophils

and macrophages) and activated endothelial cells can produce more cytokine (esp.IL-1, 6 and TNF-α,) which amplifies the inflammatory response. All these vascular pre-conditioning events can contribute to the recruitment and retention of an inflammatory infiltrate after cryosurgery.

It has been recently reported that apoptosis was observed at the edge of the cryolesion 24 hours post cryosurgery [50]. Our results are consistent with this evidence and show significant caspase activation after cryosurgery that can be further enhanced by TNF-α pre-treatment. Importantly, caspase activity was mainly found in leukocyte and endothelial cells as confirmed by co-localization of caspase 3 and CD31 staining (Fig. 5C), whereas minimal caspase activation was found in tumor cells as described in previous work [53]. This suggests that apoptosis is an outcome of endothelial cell injury due to leukocyte-endothelial cell interaction. This is supported by our previous inhibition study that showed that NFκB inhibition, rather than caspase inhibition, significantly reduced the extent of vascular injury post TNF-α enhancement of cryosurgery [26]. The caspase activation within endothelial cells is likely induced by free radicals and proteases released from infiltrating leukocytes [39]. These molecules promote apoptosis of endothelial cells, thereby leading to microvascular damage and subsequent blood flow defects [12,28]. This enhanced endothelial injury by the inflammatory infiltrate is therefore a result, but not a determinant of, vascular injury and stasis at the cryolesion edge.

An advantage of cryosurgery often cited is that of rapid wound healing and minimal scarring. This has been observed in the management of a wide variety of skin lesions, particularly those affecting the face and skin [36,52]. However, wound healing after tumor cryoablation has been less studied. Pre-treatment with TNF-α not only increased the inflammatory infiltrate and the eradication of tumor, but also advanced the initiation of granulation tissue, consisting of endothelial cells, macrophages, and fibroblasts infiltrating to the wound site. This may be due to the fact that TNF-α can stimulate active neutrophils and macrophages [30], angiogenesis [34] and enhance invasive migration of normal fibroblasts [51,57], therefore promoting the cellular activity during wound healing. In addition, the local environment (cytokines, chemokines and growth factors) modified by TNF-α stimulation can also activate a large transcriptional program, which produces cytokines and growth factors required by wound healing [12,35,55]. However, TNF-α promoted wound healing which enhances angiogenesis thereby causing infiltration of tumor cells into the cryolesion site and even recurrence and metastasis of the tumor post cryosurgery [32]. In order to better understand the effect of TNF-α on wound healing (or recurrence), future studies will need to explore time points beyond 7 days possibly using a hindlimb tumor system that allows long term growth delay and wound involution to be measured [20,25].

The innate immune response is also enhanced by TNF-α and is essential in the development of an adaptive immune response to target the cryotreated tumor [8,17,31,48]. The adaptive immune response begins with antigen uptake and presentation on antigen presenting cells (macrophages and dendritic cells) for recognition by antigen-specific T cells. However, in this study, an athymic mouse model with defective T lymphocyte production was used. Thus, while the innate immune response in our study was vigorous and dominated by neutrophils and macrophages, the contribution of the adaptive immune cells to tissue destruction was underestimated. Future investigation of the effect of TNF-α on adaptive immune response during and after cryosurgery with an immune competent animal model is clearly needed.

In conclusion, these results show the tremendous potential of TNF-α to pre-condition the vascular and immune response of a tumor thereby enhancing cryosurgical efficacy. A strong

enhancement of the inflammatory infiltrate within the cryolesion occurred due to TNF-α vascular pre-conditioning. The interaction of this infiltrate with the tumor endothelium and parenchymal cells through a blocking susceptible NFκB regulated (inflammatory) pathway is thought to be the dominant mechanism of cryosurgical injury and enhancement [26]. Apoptosis was also enhanced by TNF-α; however, this occurred subsequent to the recruitment of an inflammatory infiltrate and, due to the inability to block the effect, is not considered a dominant pathway of cryosurgical injury or enhancement [26]. Finally, granulation tissue formed after cryosurgery is also enhanced by TNF-α pre-treatment, suggesting promotion of wound healing. Further studies are still needed to elucidate the role of TNF-α in the wound healing and adaptive immune response after combinatorial cryosurgery.

Acknowledgments

Financial Support: Institute for Engineering in Medicine, University of Minnesota; NIH, R01 NCI CA07528

Institute for Engineering in Medicine, University of Minnesota; NIH RO1 NCl CA07528 for financial support.

Abbreviations

DSFC	dorsal skin fold chamber
Me2SO	dimethyl sulfoxide
VCAM	vascular cell adhesion molecule-1
H&E	hematoxylin-eosin
IHC	immunohistochemistry

References

1. Baeuerle PA, Baichwal VR. NF-kappa B as a frequent target for immunosuppressive and anti-inflammatory molecules. Adv Immunol 1997;(65):111–37. [PubMed: 9238509]
2. Bassukas ID, Gamvroulia C, Zioga A, Nomikos K, Fotika C. Cryosurgery during topical imiquimod: a successful combination modality for lentigo maligna. Int J Dermatol 2008;(47):519–21. [PubMed: 18412875]
3. Blankenstein T, Qin ZH, Uberla K, Muller W, Rosen H, Volk HD, Diamantstein T. Tumor suppression after tumor cell-targeted tumor necrosis factor alpha gene transfer. J Exp Med 1991;(173):1047–52. [PubMed: 2022919]
4. Chao BH, He X, Bischof JC. Pre-treatment inflammation induced by TNF-alpha augments cryosurgical injury on human prostate cancer. Cryobiology 2004;(49):10–27. [PubMed: 15265713]
5. Clarke DM, Baust JM, Van Buskirk RG, Baust JG. Chemo-cryo combination therapy: an adjunctive model for the treatment of prostate cancer. Cryobiology 2001;(42):274–85. [PubMed: 11748936]
6. Clarke DM, Baust JM, Van Buskirk RG, Baust JG. Addition of anticancer agents enhances freezing-induced prostate cancer cell death: implications of mitochondrial involvement. Cryobiology 2004;(49):45–61. [PubMed: 15265716]
7. Clarke DM, Robilotto AT, VanBuskirk RG, Baust JG, Gage AA, Baust JM. Targeted induction of apoptosis via TRAIL and cryoablation: a novel strategy for the treatment of prostate cancer. Prostate Cancer Prostatic Dis 2007;(10):175–84. [PubMed: 17297503]
8. Clynes R, Takechi Y, Moroi Y, Houghton A, Ravetch JV. Fc receptors are required in passive and active immunity to melanoma. Proc Natl Acad Sci U S A 1998;(95):652–6. [PubMed: 9435247]
9. Collins T, Read MA, Neish AS, Whitley MZ, Thanos D, Maniatis T. Transcriptional regulation of endothelial cell adhesion molecules: NF-kappa B and cytokine-inducible enhancers. FASEB J 1995;(9):899–909. [PubMed: 7542214]

10. Diacovo TG, Catalina MD, Siegelman MH, von Andrian UH. Circulating activated platelets reconstitute lymphocyte homing and immunity in L-selectin-deficient mice. J Exp Med 1998;(187):197–204. [PubMed: 9432977]
11. Eming SA, Krieg T, Davidson JM. Inflammation in wound repair: molecular and cellular mechanisms. J Invest Dermatol 2007;(127):514–25. [PubMed: 17299434]
12. Eppihimer MJ, Granger DN. Ischemia/reperfusion-induced leukocyte-endothelial interactions in postcapillary venules. Shock 1997;(8):16–25. [PubMed: 9249908]
13. Fletcher SG, Theodorescu D. Surgery or radiation: what is the optimal management for locally advanced prostate cancer? Can J Urol 2005;12(Suppl 1):58–61. discussion 101–2. [PubMed: 15780168]
14. Forest V, Peoc'h M, Ardiet C, Campos L, Guyotat D, Vergnon JM. In vivo cryochemotherapy of a human lung cancer model. Cryobiology 2005;(51):92–101. [PubMed: 15963488]
15. Forest V, Peoc'h M, Campos L, Guyotat D, Vergnon JM. Benefit of a combined treatment of cryotherapy and chemotherapy on tumour growth and late cryo-induced angiogenesis in a non-small-cell lung cancer model. Lung Cancer 2006;(54):79–86. [PubMed: 16889870]
16. Gage AA, Baust J. Mechanisms of tissue injury in cryosurgery. Cryobiology 1998;(37):171–86. [PubMed: 9787063]
17. Gazzaniga S, Bravo A, Goldszmid SR, Maschi F, Martinelli J, Mordoh J, Wainstok R. Inflammatory changes after cryosurgery-induced necrosis in human melanoma xenografted in nude mice. J Invest Dermatol 2001;(116):664–71. [PubMed: 11348453]
18. Glasgow SC, Ramachandran S, Csontos KA, Jia J, Mohanakumar T, Chapman WC. Interleukin-1beta is prominent in the early pulmonary inflammatory response after hepatic injury. Surgery 2005;(138):64–70. [PubMed: 16003318]
19. Goel R, Anderson K, Slaton J, Schmidlin F, Vercellotti G, Belcher J, Bischof JC. Adjuvant approaches to enhance cryosurgery. J Biomech Eng 2009;(131):074003. [PubMed: 19640135]
20. Goel R, Swanlund D, Coad J, Paciotti GF, Bischof JC. TNF-alpha-based accentuation in cryoinjury--dose, delivery, and response. Molecular cancer therapeutics 2007;(6):2039–47. [PubMed: 17620433]
21. Han B, Swanlund DJ, Bischof JC. Cryoinjury of MCF-7 human breast cancer cells and inhibition of post-thaw recovery using TNF-alpha. Technol Cancer Res Treat 2007;(6):625–34. [PubMed: 17994793]
22. Havell EA, Fiers W, North RJ. The antitumor function of tumor necrosis factor (TNF), I. Therapeutic action of TNF against an established murine sarcoma is indirect, immunologically dependent, and limited by severe toxicity. J Exp Med 1988;(167):1067–85. [PubMed: 3351434]
23. Hieber U, Heim ME. Tumor necrosis factor for the treatment of malignancies. Oncology 1994;(51):142–53. [PubMed: 8196898]
24. Hoffmann NE, Bischof JC. Cryosurgery of normal and tumor tissue in the dorsal skin flap chamber: Part II--injury response. J Biomech Eng 2001;(123):310–6. [PubMed: 11563755]
25. Jiang J, Bischof J. Effect of timing, dose and interstitial versus nanoparticle delivery of tumor necrosis factor alpha in combinatorial adjuvant cryosurgery treatment of ELT-3 uterine fibroid tumor. Cryo Letters (31):50–62.
26. Jiang J, Goel R, Iftekhar MA, Visaria R, Belcher JD, Vercellotti GM, Bischof JC. Tumor necrosis factor-alpha-induced accentuation in cryoinjury: mechanisms in vitro and in vivo. Mol Cancer Ther 2008;(7):2547–55. [PubMed: 18723499]
27. Jones JS, Rewcastle JC, Donnelly BJ, Lugnani FM, Pisters LL, Katz AE. Whole gland primary prostate cryoablation: initial results from the cryo on-line data registry. J Urol 2008;(180):554–8. [PubMed: 18550117]
28. Jordan JE, Zhao ZQ, Vinten-Johansen J. The role of neutrophils in myocardial ischemia-reperfusion injury. Cardiovasc Res 1999;(43):860–78. [PubMed: 10615413]
29. Katz AE, Rewcastle JC. The current and potential role of cryoablation as a primary therapy for localized prostate cancer. Curr Oncol Rep 2003;(5):231–8. [PubMed: 12667421]
30. Klebanoff SJ, Vadas MA, Harlan JM, Sparks LH, Gamble JR, Agosti JM, Waltersdorph AM. Stimulation of neutrophils by tumor necrosis factor. J Immunol 1986;(136):4220–5. [PubMed: 3009619]

31. Korbelik M. PDT-associated host response and its role in the therapy outcome. Lasers Surg Med 2006;(38):500–8. [PubMed: 16634073]
32. Kuszyk BS, Corl FM, Franano FN, Bluemke DA, Hofmann LV, Fortman BJ, Fishman EK. Tumor transport physiology: implications for imaging and imaging-guided therapy. AJR Am J Roentgenol 2001;(177):747–53. [PubMed: 11566666]
33. Le Pivert P, Haddad RS, Aller A, Titus K, Doulat J, Renard M, Morrison DR. Ultrasound guided combined cryoablation and microencapsulated 5-Fluorouracil inhibits growth of human prostate tumors in xenogenic mouse model assessed by luminescence imaging. Technol Cancer Res Treat 2004;(3):135–42. [PubMed: 15059019]
34. Leibovich SJ, Polverini PJ, Shepard HM, Wiseman DM, Shively V, Nuseir N. Macrophage-induced angiogenesis is mediated by tumour necrosis factor-alpha. Nature 1987;(329):630–2. [PubMed: 2443857]
35. Lentsch AB, Ward PA. Regulation of inflammatory vascular damage. J Pathol 2000;(190):343–8. [PubMed: 10685068]
36. Leopard PJ. Cryosurgery for facial skin lesions. Proc R Soc Med 1975;(68):606–8. [PubMed: 1208504]
37. Manna PP, Mohanakumar T. Human dendritic cell mediated cytotoxicity against breast carcinoma cells in vitro. J Leukoc Biol 2002;(72):312–20. [PubMed: 12149422]
38. Manson PN, Jesudass R, Marzella L, Bulkley GB, Im MJ, Narayan KK. Evidence for an early free radical-mediated reperfusion injury in frostbite. Free Radic Biol Med 1991;(10):7–11. [PubMed: 2050298]
39. Michiels C, Arnould T, Remacle J. Endothelial cell responses to hypoxia: initiation of a cascade of cellular interactions. Biochim Biophys Acta 2000;(1497):1–10. [PubMed: 10838154]
40. Mir LM, Rubinsky B. Treatment of cancer with cryochemotherapy. Br J Cancer 2002;(86):1658–60. [PubMed: 12085219]
41. Muldrew K, Rewcastle J, Donnelly BJ, Saliken JC, Liang S, Goldie S, Olson M, Baissalov R, Sandison G. Flounder antifreeze peptides increase the efficacy of cryosurgery. Cryobiology 2001;(42):182–9. [PubMed: 11578117]
42. Ozer K, Adanali G, Siemionow M. Late effects of TNF-alpha-induced inflammation on the microcirculation of cremaster muscle flaps under intravital microscopy. J Reconstr Microsurg 2002;(18):37–45. [PubMed: 11917955]
43. Papenfuss HD, Gross JF, Intaglietta M, Treese FA. A transparent access chamber for the rat dorsal skin fold. Microvasc Res 1979;(18):311–8. [PubMed: 537508]
44. Partheniou F, Kelsey SM, Srinivasula SM, Newland AC, Alnemri ES, Jia L. c-IAP1 blocks TNFalpha-mediated cytotoxicity upstream of caspase-dependent and -independent mitochondrial events in human leukemic cells. Biochem Biophys Res Commun 2001;(287):181–9. [PubMed: 11549272]
45. Pease GR, Wong ST, Roos MS, Rubinsky B. MR image-guided control of cryosurgery. J Magn Reson Imaging 1995;(5):753–60. [PubMed: 8748498]
46. Pham L, Dahiya R, Rubinsky B. An in vivo study of antifreeze protein adjuvant cryosurgery. Cryobiology 1999;(38):169–75. [PubMed: 10191041]
47. Rubinsky B. Cryosurgery. Annu Rev Biomed Eng 2000;(2):157–87. [PubMed: 11701510]
48. Sabel MS. Cryo-immunology: a review of the literature and proposed mechanisms for stimulatory versus suppressive immune responses. Cryobiology 2009;(58):1–11. [PubMed: 19007768]
49. Saliken JC, Donnelly BJ, Rewcastle JC. The evolution and state of modern technology for prostate cryosurgery. Urology 2002;(60):26–33. [PubMed: 12206845]
50. Schacht V, Becker K, Szeimies RM, Abels C. Apoptosis and leucocyte-endothelium interactions contribute to the delayed effects of cryotherapy on tumours in vivo. Arch Dermatol Res 2002;(294):341–8. [PubMed: 12420102]
51. Schirren CG, Scharffetter K, Hein R, Braun-Falco O, Krieg T. Tumor necrosis factor alpha induces invasiveness of human skin fibroblasts in vitro. J Invest Dermatol 1990;(94):706–10. [PubMed: 2324525]
52. Shepherd JP, Dawber RP. Wound healing and scarring after cryosurgery. Cryobiology 1984;(21):157–69. [PubMed: 6713945]

53. Steinbach JP, Weissenberger J, Aguzzi A. Distinct phases of cryogenic tissue damage in the cerebral cortex of wild-type and c-fos deficient mice. Neuropathol Appl Neurobiol 1999;(25):468–80. [PubMed: 10632897]
54. Szpaderska AM, Egozi EI, Gamelli RL, DiPietro LA. The effect of thrombocytopenia on dermal wound healing. J Invest Dermatol 2003;(120):1130–7. [PubMed: 12787144]
55. Theilgaard-Monch K, Knudsen S, Follin P, Borregaard N. The transcriptional activation program of human neutrophils in skin lesions supports their important role in wound healing. J Immunol 2004;(172):7684–93. [PubMed: 15187151]
56. Udagawa M, Kudo-Saito C, Hasegawa G, Yano K, Yamamoto A, Yaguchi M, Toda M, Azuma I, Iwai T, Kawakami Y. Enhancement of immunologic tumor regression by intratumoral administration of dendritic cells in combination with cryoablative tumor pretreatment and Bacillus Calmette-Guerin cell wall skeleton stimulation. Clin Cancer Res 2006;(12):7465–75. [PubMed: 17189420]
57. Vilcek J, Palombella VJ, Henriksen-DeStefano D, Swenson C, Feinman R, Hirai M, Tsujimoto M. Fibroblast growth enhancing activity of tumor necrosis factor and its relationship to other polypeptide growth factors. J Exp Med 1986;(163):632–43. [PubMed: 3512757]
58. Vos IH, Govers R, Grone HJ, Kleij L, Schurink M, De Weger RA, Goldschmeding R, Rabelink TJ. NFkappaB decoy oligodeoxynucleotides reduce monocyte infiltration in renal allografts. FASEB J 2000;(14):815–22. [PubMed: 10744638]
59. Walter Schurch, TAS.; Gabbiani, Giulio. Histology for Pathologists. Philadelphia: Lippincott-Raven Publishers; 1997.
60. Weiss SJ. Tissue destruction by neutrophils. N Engl J Med 1989;(320):365–76. [PubMed: 2536474]
61. Yuan F, Zhou W, Zhang J, Zhang Z, Zou C, Huang L, Zhang Y, Dai Z. Anticancer drugs are synergistic with freezing in induction of apoptosis in HCC cells. Cryobiology 2008;(57):60–5. [PubMed: 18586021]

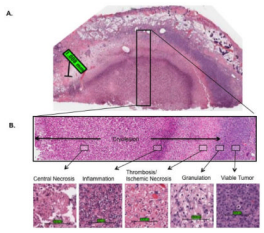

Figure 1.

Five histological zones were evident after cryosurgery: central necrosis, inflammation, thrombosis/ischemic necrosis, granulation tissue influx, and viable tumor. (A) Demonstration of these histological zones at day 3 post cryosurgery (20× objective; scale bar = 1mm). (B) Demonstration of these histological zones at 40× objective magnification (scale bar = 100 μm).

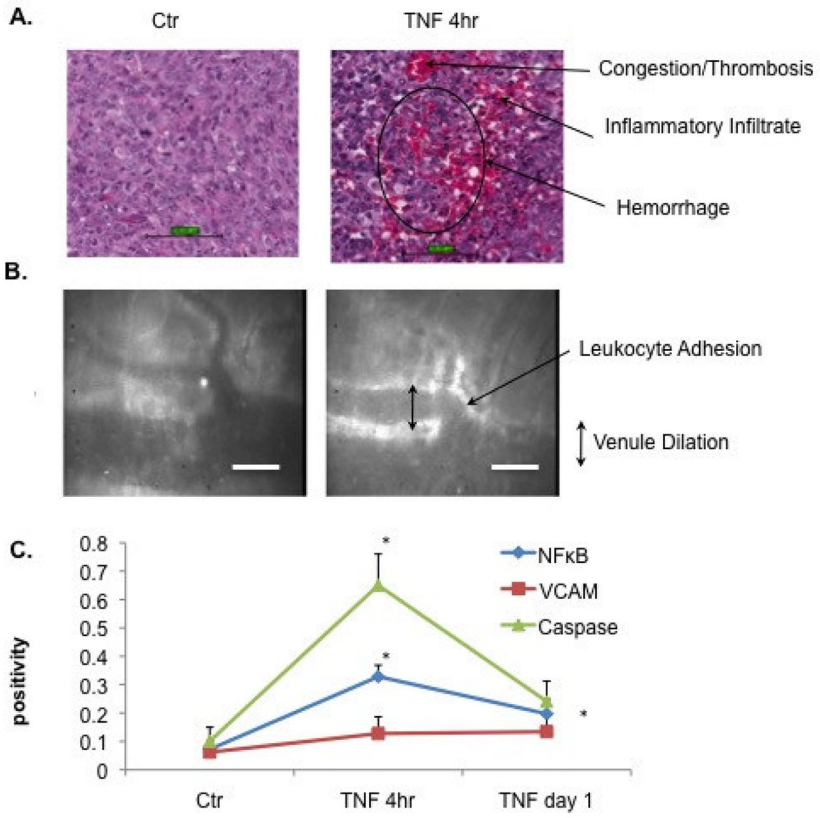

Figure 2.

TNF-α treatment mediated vascular pre-conditioning events. (A) TNF-α induced histological changes in tumor tissue including congestion/thrombosis, inflammatory infiltrate and hemorrhage (scale bar = 100 μm). (B) TNF-α resulted in microvascular dilatation and enhanced leukocyte association with vessel walls, as visualized by intravital fluorescent videotaping after intravenous administration of the nuclear dye rhodamine 6G (scale bar = 100 μm). (C) TNF-α induced caspase activation in tumor and endothelial cells at 4 hours after treatment (*, $p<0.05$), and NFκB activation in endothelial cells at 4 hours and day 1 after treatment (*, $p<0.05$). Data are presented as the mean (bar height = 1 standard deviation) of three to four independent experiments for each treatment.

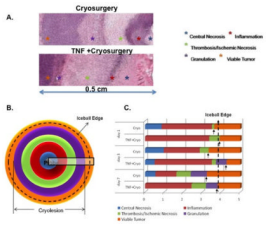

Figure 3.

Dynamic histological changes following cryosurgery with/without TNF-α pre-treatment. (A) TNF-α modified histological layers at day 7 post cryosurgery as compare to cryosurgery alone in tumor tissue. (B) Representation of the iceball formation and five histological zones following cryosurgery (see Fig. 1). (C) Demonstration of changes in the normalized radii of histological zones over time (bar values represent the mean of three to four independent experiments for each treatment; see Table 2 for the mean and standard deviation). Arrows represent histologic cryolesion edge (boundaries of granulation tissue zone) for illustration. Dashed arrows indicate the iceball edge (3.9 mm, −0.5°C) [20].

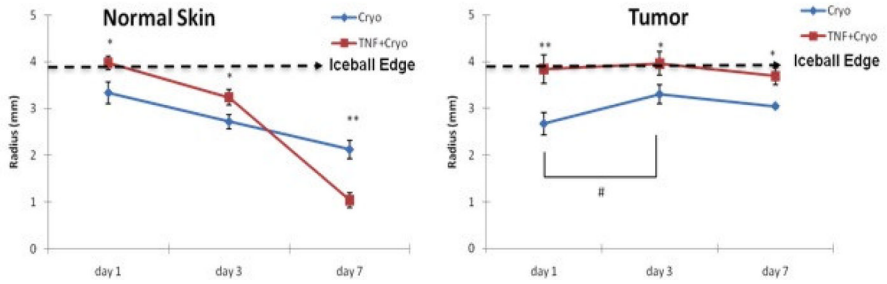

Figure 4.

Stasis radius at days 1, 3 and 7 after cryosurgery measured by intravital microscopic imaging following FITC-dextran injection. Stasis radius was significantly enhanced by TNF-α pre-treatment combined with cryosurgery as compared to cryosurgery alone (*, $p<0.05$; **, $p<0.001$). For tumor tissue cryosurgery alone, extension of stasis radius was observed from day 1 to day 3 (#, $p<0.05$). The bar values represent Mean ± SD of at least four independent experiments for each treatment. Dashed arrows indicate the iceball edge (3.9mm, −0.5°C).

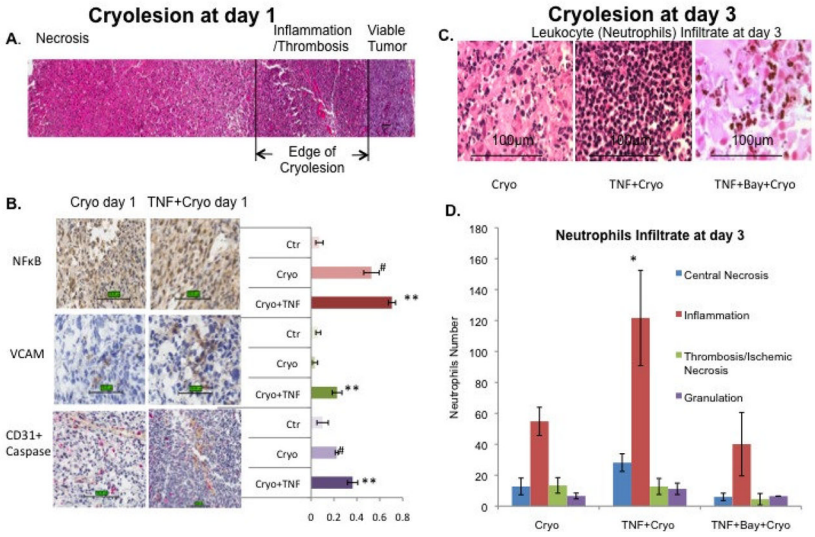

Figure 5.

Molecular and cellular mechanisms of TNF-α enhanced cryosurgery. (A) Immunohistochemical demonstration of NFκB, VCAM and caspase 3 (red) and CD31 (brown) activation at the edge of the cryolesion at day 1 post cryosurgery (scale bar=100μm). (B) Quantitative immunohistochemistry of NFκB, VCAM and caspase 3 signal in the cryolesion at day 1 post cryosurgery. The average number of positive pixels/total pixels was derived from five representative fields within each sample; values represent mean ± SD of three to four independent experiments for each treatment; there were statistically significant ($p<0.05$) differences between cryosurgery versus sham control (#), and combinatorial treatment versus cryosurgery alone (**). (C) Leukocyte (neutrophils) infiltrate at day 3 post cryosurgery with or without TNF-α pre-treatment. Animals were treated with cryosurgery alone, TNF-α 4 hours pre-treatment plus cryosurgery, or NFκB inhibitor Bay followed by TNF-α 4 hours pre-treatment plus cryosurgery. Representative image of neutrophilic infiltrate with H&E staining was taken under high power (100× magnification) within the inflammation zone (scale bar =100μm). (D) Quantification of neutrophils within leukocyte infiltrate within each histological zone under high power field. The average number of neutrophils was measured in five representative fields in each histological layer for each sample. The bar values represent mean ± SD of three to four independent experiments for each treatment. The numbers of neutrophils per field were significantly different between the combinatorial treatment and cryosurgery alone (*, $p<0.05$).

Table 1

Time course of morphologic changes post TNF-α treatment[a]

Time post-treatment	Inflammatory infiltrate[b]	Hemorrhage[c]	Thrombosis & Congestion[d]	Tumor Necrosis[e]
Ctr	-	-	-	-
4hr	++++	+++	++	+
Day 1	+++	-	++	+++
Day 3	+	-	+	+++
Day 7	+	-	+	++

[a] Data correspond to semi-quantitative evaluation in tumor areas of hematoxylin-eosin sections (evaluation was made in five representative fields per sample under $20^{\times}$ magnification]. Three to four independent experiments were performed for each treatment.

[b] Average numbers of leukocytes per field.

[c] Percent of tissue area involved by hemorrhage.

[d] Average number of vessels affected by congestion/dilation and thrombosis per field.

[e] Percent of tumor area involved by necrosis.

Table 2

Quantitative measurements of the radius of histological zones following cryosurgery

Treatment		Vascular Stasis[b]	Cryolesion (Histology)[c]	Central Necrosis[d]	Inflammation[d]	Thrombosis /ischemic necrosis[d]	Granulation[d]	Viable Tumor[d]
Day 1	Cryo	2.7±0.7	e	0.9±0.6	2.6±0.9	0.1±0.1	NA	1.4±0.3
	TNF+Cryo	3.8±0.8*	3.9±0.6	NA	3.4±0.6	0.5±0.5	NA	1.1±0.2
Day 3	Cryo	3.3±0.5#	3.3±0.6	1.0±0.7	1.9±0.8	0.5±0.4	NA	1.7±0.6
	TNF+Cryo	4.0±0.4*	4.3±0.3*	0.5±0.9	3.0±0.5*	0.2±0.2	0.6±0.5	0.7±0.3*
Day 7	Cryo	3.1±0.1	3.2±0.4	0.5±0.3	1.1±0.7	0.7±0.5	0.8±0.3	1.8±0.4
	TNF+Cryo	3.7±0.5*	3.8±0.5*	NA	2.4±0.5*	0.8±0.4	0.6±0.5	1.2±0.5*

[a] The values represent Mean ± SD of three to four Independent experiments for each treatment.

[b] Radius of vascular stasis was measured by intravital microscopic imaging following FITC-dextran injection.

[c] Radii of granulation tissue (outer bound of cryolesion) were measured from digitized H&E-stained sections (corrected for tissue shrinkage after histologic processing as described in Materials and Methods).

[d] Radii of histological zones of central necrosis, inflammation, thrombosis/ischemic necrosis, granulation tissue influx, and viable tumor were measured from digitized H&E-stained sections (corrected for tissue shrinkage after histologic processing as described in Materials and Methods).

[e] Cryolesion edge at day 1 after cryosurgery is imperceptible based on H&E-stained sections.

[#] There was a significant change ($p<0.05$) in radius of vascular stasis from day 1 to day 3 as measured by intravital microscopic imaging.

[*] Significant changes ($p<0.05$) between combinatorial (TNF-a + cryosurgery) therapy versus cryosurgery alone were seen in the radii of vascular stasis measured by intravital microscopic imaging, and in radii of histologic zones following cryosurgery.